

Article

Two Interpenetrated Zn(II) Coordination Polymers: Synthesis, Topological Structures, and Property

Zi-Wei He, Chang-Jie Liu, Wei-Dong Li, Shuai-Shuai Han and Shui-Sheng Chen * 

School of Chemistry and Chemical Engineering, Fuyang Normal University, Fuyang 236041, China; heziwei990208@tom.com (Z.-W.H.); liuchangjie990519@tom.com (C.-J.L.); lwd18856859717@tom.com (W.-D.L.); hanshuaishuai@tom.com (S.-S.H.)

* Correspondence: fyuniv@163.com; Tel.: +86-558-259-5836

Received: 1 November 2019; Accepted: 14 November 2019; Published: 17 November 2019



Abstract: Two interpenetrated coordination polymers (CPs) $\{[\text{Zn1}(\text{L})(\text{NO}_2\text{pbda})]_n[\text{Zn2}(\text{L})(\text{NO}_2\text{pbda})]_n\}$ (**1**) and $[\text{Zn}(\text{L})(\text{Brpbda})]_n$ (**2**) were prepared by reactions of zinc sulfate heptahydrate with N-donor ligands of 1,4-di(1*H*-imidazol-4-yl)benzene (L) and auxiliary carboxylic acids of nitroterephthalic acid ($\text{H}_2\text{NO}_2\text{pbda}$) and 2,5-dibromoterephthalic acid (H_2Brpbda), respectively. The structures of the CPs were characterized by Fourier-Transform Infrared (IR) spectroscopy, elemental analysis, and single-crystal X-ray diffraction. The coordination polymer **1** has two different (4, 4) **sql** 2D layer structures based on the $[\text{Zn}(\text{L})(\text{NO}_2\text{pbda})]$ moiety, which results in inclined interpenetration with a 2D + 2D \rightarrow 3D architecture, while the CP **2** exhibits a 3-fold interpenetrating **dmp** network. The diffuse reflectance spectra are also investigated for the CPs **1** and **2**.

Keywords: coordination polymers; structures; diffuse reflectance spectra

1. Introduction

The design of metal–organic coordination polymers (CPs), as one of the most active research areas, has acquired great attention in recent years, due to their intriguing structures and significant applications [1–7]. Recently, luminescent coordination polymers have been widely employed to detect guest molecules with high sensitivity and selectivity. For example, two CPs, $\{[\text{Cd}_2\text{L}_2(\text{H}_2\text{O})_4] \cdot \text{H}_2\text{O}\}_n$ and $\{[\text{Zn}_2\text{L}_2(\text{H}_2\text{O})_4] \cdot \text{H}_2\text{O}\}_n$ ($\text{H}_2\text{L} = 5\text{-}(1\text{H}\text{-}1,2,4\text{-triazol-}1\text{-yl})\text{isophthalic acid}$), can serve as highly selective and sensitive fluorescent probes toward Cr^{VI} -anions (CrO_4^{2-} and $\text{Cr}_2\text{O}_7^{2-}$) [8]. In crystal engineering, the most important factors in assembling desirable CPs are the rational choosing of the bridging ligand and metal centers; in addition, other reaction conditions, such as solvent, temperature, pH value, and the nature of anions, can affect the resulting framework [9–13]. It should be mentioned that the length, rigidity, functional groups, coordination modes, or substituents of organic ligands can decide the final frameworks of CPs [14,15]. Generally, two important kinds of ligands, including N-donor and O-donor organic compounds, are widely used to construct diverse CPs, due to their various coordination modes and modifiable backbones [16,17]. Noticeably, rigid rod-type ligands, including 4,4'-bipyridine (bpy), terephthalic acid, or their analogues, often act as pillars in building a rich variety of new entangled CPs [18,19], while the flexible ligands have different shapes associated with the trans or gauche conformation, favoring the formation of interesting entanglements [20,21]. More recently, a new type of rigid N-donor ligand, including the 4-imidazolyl group, has been designed by our group, and employed to fabricate porous crystalline materials with good gas adsorption properties [22–34]. Moreover, a series of diverse CPs have been built through the mixed system of imidazole and polycarboxylates [25,26]. Taking into account their good compatibility for the N/O donor mixed system, we choose different carboxylic acids with distinct natures, together with the rigid rod-type 1,4-di(1*H*-imidazol-4-yl)benzene (L) ligand to build novel CPs as our continual

work. In this contribution, we report two Zn(II) CPs of $\{[Zn1(L)(NO_2pbda)]_n[Zn2(L)(NO_2pbda)]_n\}$ (**1**) and $[Zn(L)(Brpbda)]$ (**2**) by reactions of zinc sulfate heptahydrate with mixed ligands of L and nitroterephthalic acid (H_2NO_2pbda), and 2,5-dibromoterephthalic acid ($H_2Brpbda$), respectively.

2. Materials and Methods

2.1. Materials and Techniques

The L organic ligand was synthesized according to the literature [27]. The infrared spectrum was recorded on a Bruker Vector 22 FTIR spectrophotometer (Instrument Inc., Karlsruhe, Germany). Elemental analyses were performed on a PerkinElmer 2400 elemental analyzer (PerkinElmer, Waltham, MA, USA). The UV-vis spectra were recorded using a computer-controlled PE Lambda 900 UV-vis spectrometer (PerkinElmer, USA). Thermogravimetric analyses (TGA) were analyzed by a simultaneous SDT 2960 thermal analyzer (Thermal Analysis Instrument Inc., New Castle, DE, USA). Power X-ray diffraction (PXRD) patterns were measured on a Shimadzu XRD-6000 X-ray diffractometer (Shimadzu Corporation, Kyoto, Japan) with $CuK\alpha$ ($\lambda = 1.5418 \text{ \AA}$) radiation.

2.2. Synthesis of $\{[Zn1(L)(NO_2pbda)]_n[Zn2(L)(NO_2pbda)]_n\}$ (**1**)

Mixtures of $ZnSO_4 \cdot 7H_2O$ (28.7 mg, 0.1 mmol), L (21.2 mg, 0.1 mmol), H_2NO_2pbda (21.1 mg, 0.1 mmol), and H_2O (10 mL) were adjusted to pH = 7 with an NaOH solution (0.2 mol L^{-1}), and were placed in a 25 mL Teflon-lined container and heated to $160 \text{ }^\circ\text{C}$ for 72 h. Brown block crystals of **1** were collected, with a yield of 69%, at room temperature. Anal. calcd for $C_{20}H_{13}N_5O_6Zn$ (%): C, 49.56; H, 2.70; N, 14.45. Found: C, 49.38; H, 2.56; N, 14.62. IR: 3447 (w), 3141 (w), 1628 (vs), 1528 (s), 1488 (m), 1377 (m), 1346 (vs), 1264 (w), 1179 (w), 1124 (w), 1073 (w), 948 (w), 837 (m), 816 (m), 785 (w), 651 (w), 612 (w), 521 (w), 489 (w), 421 (w).

2.3. Synthesis of $[Zn_2(L)(Brpbda)_2]_n$ (**2**)

The same synthetic method as above was used, except that H_2NO_2pbda was replaced by $H_2Brpbda$ (32.4 mg, 0.01 mmol). Brown block crystals of **2** were obtained (yield: 61%). Anal. calcd for $C_{20}H_{10}Br_2N_4O_4Zn$ (%): C, 40.34; H, 1.69; N, 9.41. Found: C, 40.19; H, 1.75; N, 9.29. IR: 3465 (m), 3386 (m), 3126 (m), 2856 (m), 1638 (s), 1581 (s), 1545 (s), 1489 (m), 1412 (s), 1359 (m), 1272 (w), 1182 (m), 1172 (m), 1145 (m), 1132 (s), 1081 (m), 968 (m), 838 (m), 818 (s), 798 (m), 679 (m), 648 (m), 628 (w), 530 (w), 459 (w).

2.4. Crystallographic Data Collection and Refinements

The data collection for CPs **1–2** was carried out on a Bruker Smart Apex CCD area-detector diffractometer. The diffraction data and structural analysis were integrated using the *SAINTE* program and the *SADABS* program, and anisotropically, on F^2 by the full-matrix least-squares technique, respectively [28–30]. The details of the crystal parameters are summarized in Table 1; selected bond lengths and angles are listed in Table S1. CCDC: 1959065, 1959064 for **1** and **2**. The atoms of C, O, and Br for CP **2** are disordered and split into (C5, C5B), (C6A, C6B), (C7A, C7B), (C8A, C8B), (C9A, C9B), (C10A, C10B), (O1A, O1B), (O2A, O2B), and (Br1A, Br1B). Copy of the data can be obtained free of charge on application to CCDC, 12 Union Road, Cambridge CB2 1EZ, UK (Fax: +44-1223-336-033; E-Mail: deposit@ccdc.cam.ac.uk).

Table 1. Crystallographic data and structure refinement details for coordination polymers (CPs) 1 and 2.

	1	2
Empirical formula	C ₂₀ H ₁₃ N ₅ O ₆ Zn	C ₂₀ H ₁₀ Br ₂ N ₄ O ₄ Zn
Formula weight	484.72	595.51
Temperature/K	296(2)	296(2)
Crystal system	Triclinic	Orthorhombic
Space group	<i>P</i> 1	<i>P nna</i>
<i>a</i> /Å	9.037(2)	11.0101(10)
<i>b</i> /Å	9.141(2)	14.6802(14)
<i>c</i> /Å	12.948(3)	14.8721(13)
α /°	107.832(3)	90
β /°	95.123(3)	90
γ /°	108.233(3)	90
<i>V</i> (Å ³)	946.6(4)	2403.8(4)
<i>Z</i> , <i>D</i> _{calc} /(Mg/m ³)	2, 1.701	4, 1.646
<i>F</i> (000)	492	1160
θ range/°	1.69–25.99	3.59–25.01
Reflections collected	7131	26144
Independent reflections	5942	2088
Goodness-of-fit on <i>F</i> ²	0.997	1.094
<i>R</i> ₁ [<i>I</i> > 2σ(<i>I</i>)] ^a	0.0398	0.0989
<i>wR</i> ₂ [<i>I</i> > 2σ(<i>I</i>)] ^b	0.0819	0.2401

$$^a R_1 = \sum ||F_o| - |F_c|| / \sum |F_o|. \quad ^b wR_2 = \frac{|\sum w(|F_o|^2 - |F_c|^2)|}{\sum [w(F_o)^2]^{1/2}}, \text{ where } w = 1/[\sigma^2(F_o^2) + (aP)^2 + bP]. \quad P = (F_o^2 + 2F_c^2)/3.$$

3. Results

3.1. Structural Descriptions

3.1.1. Structure of {[Zn1(L)(NO₂pbda)]_n[Zn2(L)(NO₂pbda)]_n} (1)

Single-crystal structural analysis reveals that CP 1 crystallizes in a monoclinic form with space group *P* 1 (Table 1). The asymmetric unit has two sets of [Zn(L)(NO₂pbda)] units, and each unit includes a distinct Zn(II) atom, one L ligand, and one NO₂pbda²⁻. Both of the Zn(II) atoms possess a N₂O₂ donor set, forming 4-coordinated tetrahedral coordination geometry (Figure 1a). The Zn–O bond distances range from 1.939(3) to 2.015(3) Å and the Zn–N bond distances range from 1.980(4) to 2.000(4) Å; the coordination angles around Zn(II) range from 94.83(14)° to 128.61(17)° (Table S1). Noticeably, in each independent set of [Zn(L)(NO₂pbda)]_n, the NO₂pbda²⁻ ligands act as linear ligands to link two Zn(II) atoms by the opposite carboxylate groups in the $\mu_1\text{-}\eta^1:\eta^0$ -monodentate mode, forming a one-dimensional (1D) chain [Zn(NO₂pbda)]_n. The linear L ligands connect 1D chains into two-dimensional (2D) [Zn(L)(NO₂pbda)]_n layers (Figure 1b), which can be considered as 4⁴-**sql** topology, by taking Zn(II) atoms as 4-connecting nodes, and the L and NO₂pbda²⁻ ligands as 2-connectors. Thus, two L ligands together with two NO₂pbda²⁻ units, connect four Zn(II) atoms to afford a [Zn₄(L)₂(NO₂pbda²⁻)₂] square unit, where the lateral Zn···Zn distances are around 9.10 and 13.36 Å. The rhombus has large rectangular windows, which permit inclined interpenetration for these two distinct [Zn(L)(NO₂pbda)] layers, with an angle of 66.24°, forming the 2D + 2D → 3D inclined polycatenation framework (Figure 1c,d) [31,32].

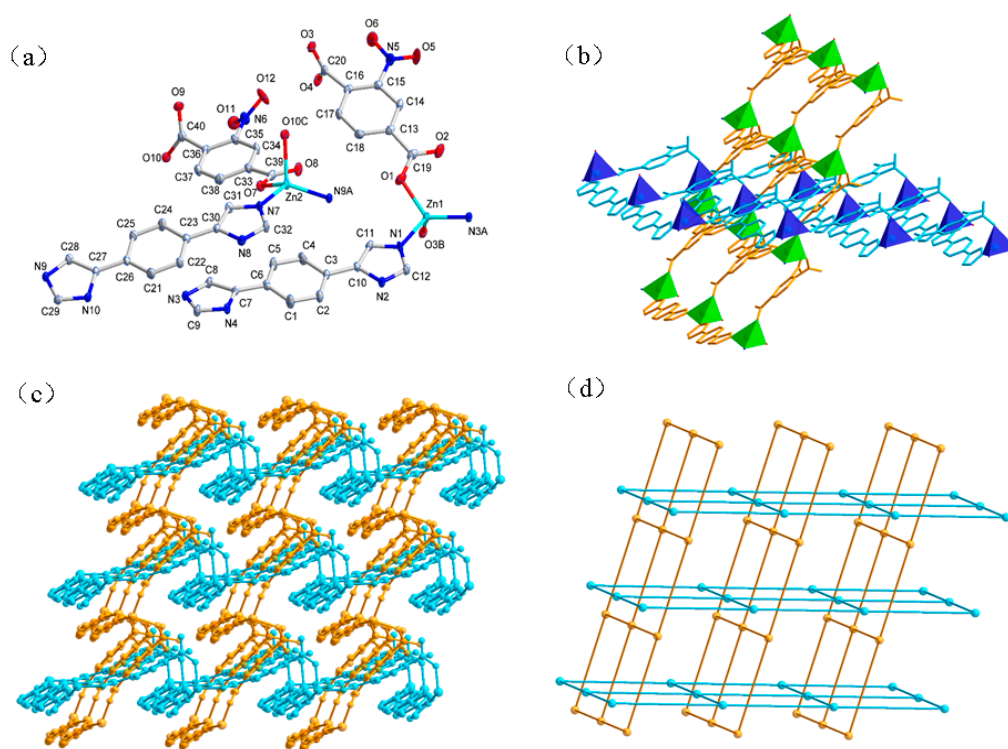


Figure 1. (a) The coordination environment of the Zn(II) atoms in **1**. Symmetry code: A $x, 1+y, 1+z$, B $-1+x, y, z$, C $x, 1+y, z$. (b) 2D polycatenation of **1**. (c) The 3D framework built from 2D + 2D \rightarrow 3D interpenetration. (d) Schematic representation of inclined interpenetration in **1**.

3.1.2. Structure of $[\text{Zn}(\text{L})(\text{Brpbda})]_n$ (**2**)

A different H_2Brpbda acid with a Br atom substituent group replaced $\text{H}_2\text{NO}_2\text{pbda}$ in the reaction of **1**, and the new compound of **2**, possessing 3-fold interpenetrating **dmp** topology was obtained. Complex **2** crystallizes in the orthorhombic $Pnna$ space group, quite different from the monoclinic space group, $P1$, in **1**. The asymmetric unit includes half of the $[\text{Zn}(\text{L})(\text{Brpbda})]$ units, namely half of a distinct Zn(II) atom, a Brpbda^{2-} anion, and an L unit, respectively. As shown in Figure 2a, the Zn1 atom is coordinated by two oxygen atoms (O1, O1A) from two different Brpbda^{2-} anions, and two nitrogen atoms (N3, N3A) of two L ligands, forming distorted tetrahedral coordination geometry. In **2**, each Brpbda^{2-} anion links two adjacent Zn^{2+} ions by two carboxyl groups using the $\mu_1-\eta^1:\eta^0$ -monodentate coordination mode, generating a 1D zigzag chain along the a axis (Figure 2b). Similarly, the linear L ligands act as 2-connectors to link Zn(II) atoms to form 1D zigzag chains. As a consequence, these 1D chains are interconnected to afford a 3D coordination framework (Figure 2c). Topologically, both the μ_2 - Brpbda^{2-} anions and the L ligands are linear 2-connectors, while each Zn(II) atom is a 4-connector to connect the other four Zn(II) atoms by two Brpbda^{2-} and two L ligands. Thus, the network of **2** is a 4-connected **dmp** net with a $(6^5 \cdot 8)$ topology [33,34]. Due to the great void of each single net, it permits the inclusion of another two independent equivalent networks, resulting in a 3-fold interpenetrating **dmp** net (Figure 2d).

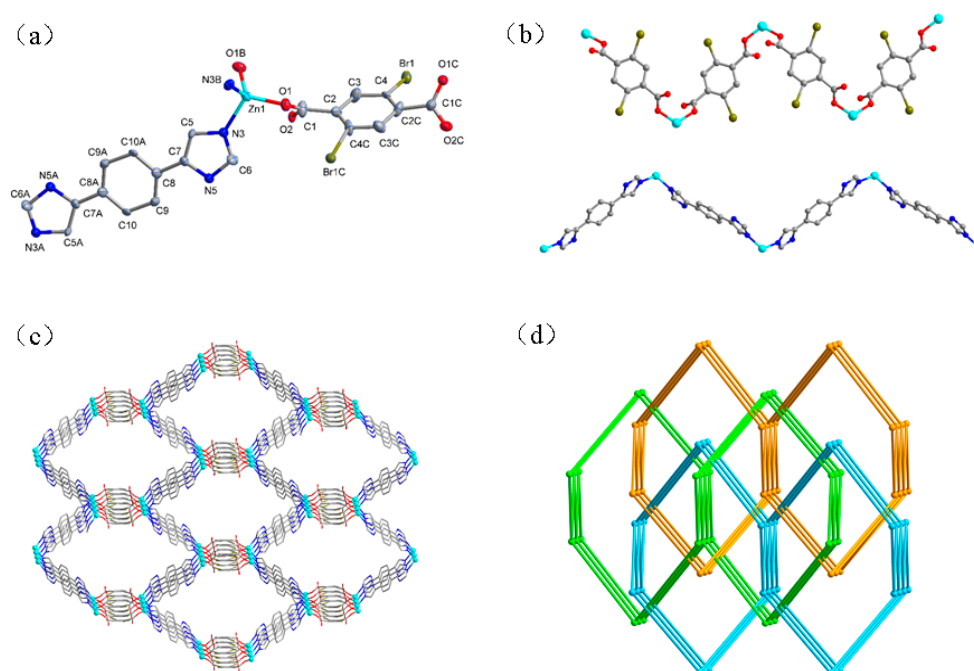


Figure 2. (a) The coordination environment of the Zn(II) atoms in **2**. Symmetry code: $A\ 2-x, 1-y, 1-z, B\ x, 0.5-y, 0.5-z, C\ 0.5-x, -y, z$. (b) 1D chains of $[Zn(II)(Brpbda^{2-})]$ and $[Zn(II)(L)]$ in **2**. (c) 3D framework of **2**. (d) Schematic representation of the 3-fold interpenetrating **dmp** net with a $(6^5 \cdot 8)$ topology.

3.2. Thermal Analyses and X-Ray Power Diffraction Analyses

The stability of CPs **1** and **2** was evaluated by thermogravimetric analysis (TGA); the analysis results are listed in Figure S1. The results of TGA for CPs **1** and **2** showed no weight losses for the crystalline materials until the frameworks collapse at about 195 and 245 °C respectively, indicating that the frameworks of compounds **1–2** contain no guest molecules, which is consistent with their structures, as evidenced by the analysis of the crystal structures. The diffraction peaks of as-synthesized CPs **1** and **2** fit well with the simulated power X-ray diffraction (PXRD) patterns from single crystal results. The result confirms that the as-synthesized crystalline materials of **1** and **2** are phase purities, as shown in Figure S2.

3.3. IR and Diffuse Reflectance Spectra

IR spectra of CPs **1** and **2** were recorded between 4000 and 400 cm^{-1} . The characteristic peak with vibrational bands, 1638–1528 cm^{-1} , disappear around 1700 cm^{-1} , which means the carboxylic groups are deprotonated. The infrared spectra of L indicate the prominent characteristic absorption bands at 1528–1489 and 1270–1124 cm^{-1} , attributed to its aromatic rings [35].

The UV–vis absorption spectra of **1** and **2** in their solid states were recorded in Figure 3. The L ligand shows intense absorption peaks ranging from 250 to 300 nm, which belongs to $\pi-\pi^*$ transitions [36]. Obviously, the CPs **1** and **2** showed similar absorption bands in the UV region, which correspond to intraligand $\pi \rightarrow \pi^*$ and $n \rightarrow \pi^*$ transitions. Furthermore, the diffuse reflectance data obtained were transformed into a Kubelka–Munk function to get their band gaps (E_g), which can be employed to evaluate the semiconductivity of the CPs. The values of E_g are estimated as 3.52 and 2.59 eV for CPs **1** and **2** (Figure 4), which were determined by a direct band gap semiconductor: $(Ah\nu)^2 = B(h\nu - E_g)$. The values of E_g for CPs **1** and **2** are comparatively a little higher than the series of Ni(II) compounds [37], and the as-synthesized crystalline materials may be optical semiconductors [38].

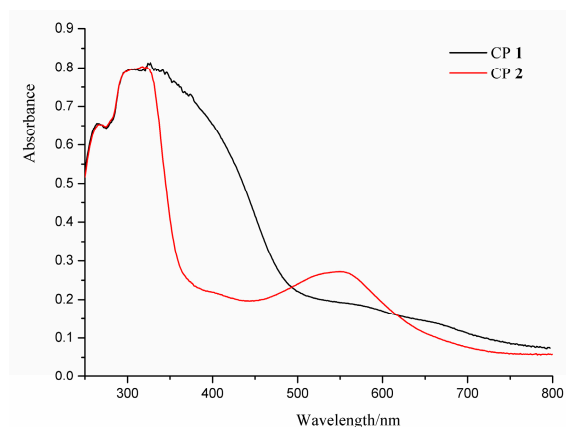


Figure 3. The UV-vis spectra for the CPs 1–2.

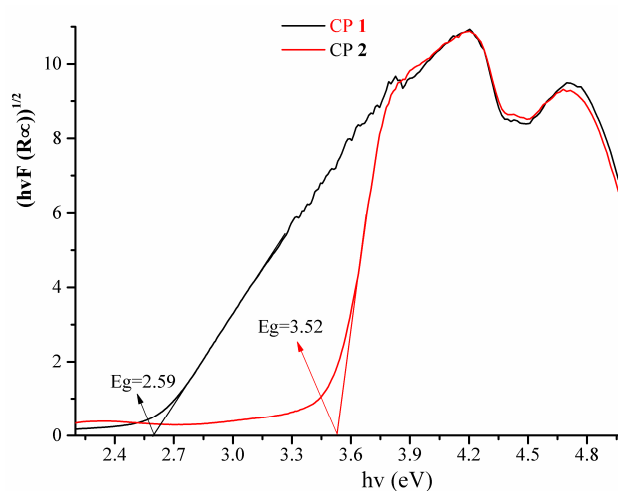


Figure 4. The E_g values for CPs 1–2 treated with the Kumble–Munk function.

4. Conclusions

Two interpenetrated Zn(II) CPs based on mixed N-donor and O-donor ligands of L and aromatic dicarboxylic acid were prepared with reactions of zinc sulfate heptahydrate by hydrothermal reaction. The natures of the different substituent groups of auxiliary dicarboxylic acid ligands make different structures for CPs 1 and 2. The compounds 1 and 2 are 2D + 2D → 3D-inclined polycatenation structures or 3-fold interpenetrating **dmp** networks, due to different substituent groups from nitroterephthalic acid and 2,5-dibromoterephthalic acid. The UV-vis absorption spectra of 1 and 2 were investigated. The results have further confirmed that the mixed system of N/O-donor ligands is a favorable strategy for building diverse coordination polymers.

Supplementary Materials: The following are available online at <http://www.mdpi.com/2073-4352/9/11/601/s1>. Figure S1 and S2 represent TGA and PXRD. Selected bond lengths and bond angles are listed in Table S1.

Author Contributions: Z.-W.H. and C.-J.L. did the experiments and analyzed the data. W.-D.L. and S.-S.H. made the measurements. S.-S.C. charged the project.

Funding: Thanks for the funding of the Cooperative Project of Fuyang Government (XDHX201707) and the youth talent program (gxbjZD19).

Conflicts of Interest: The authors declare no conflict of interest.

References

1. Kang, Y.S.; Lu, Y.; Chen, K.; Zhao, Y.; Wang, P.; Sun, W.Y. Metal-organic frameworks with catalytic centers: From synthesis to catalytic application. *Coord. Chem. Rev.* **2019**, *378*, 262–280. [CrossRef]

2. Fu, H.R.; Wang, N.; Qin, J.H.; Han, M.L.; Ma, L.F.; Wang, F. Spatial confinement of a cationic MOF: A SC-SC approach for high capacity Cr(VI)-oxyanion capture in aqueous solution. *Chem. Commun.* **2018**, *54*, 11645–11648. [[CrossRef](#)] [[PubMed](#)]
3. Zhao, Y.; Wang, L.; Fan, N.N.; Han, M.L.; Yang, G.P.; Ma, L.F. Porous Zn(II)-based metal–organic frameworks decorated with carboxylate groups exhibiting high gas adsorption and separation of organic dyes. *Cryst. Growth Des.* **2018**, *18*, 7114–7121. [[CrossRef](#)]
4. Yang, X.G.; Ma, L.F.; Yan, D.P. Facile synthesis of 1D organic–inorganic perovskite micro-belts with high water stability for sensing and photonic applications. *Chem. Sci.* **2019**, *10*, 4567–4572. [[CrossRef](#)]
5. Seidi, F.; Jenjob, R.; Crespy, D. Designing smart polymer conjugates for controlled release of payloads. *Chem. Rev.* **2018**, *118*, 3965–4036. [[CrossRef](#)]
6. Zhao, Y.; Yang, X.G.; Lu, X.M.; Yang, C.D.; Fan, N.N.; Yang, Z.T.; Wang, L.Y.; Ma, L.F. {Zn₆} cluster based metal–organic framework with enhanced room-temperature phosphorescence and optoelectronic performances. *Inorg. Chem.* **2019**, *58*, 6215–6221. [[CrossRef](#)]
7. Cheng, Y.J.; Wang, R.; Wang, S.; Xi, X.J.; Ma, L.F.; Zang, S.Q. Encapsulating [Mo₃S₁₃]²⁻ clusters in cationic covalent organic frameworks: Enhancing stability and recyclability by converting a homogeneous photocatalyst to a heterogeneous photocatalyst. *Chem. Commun.* **2018**, *54*, 13563–13566. [[CrossRef](#)]
8. Wang, C.X.; Xia, Y.P.; Yao, Z.Q.; Xu, J.; Chang, Z.; Bu, X.H. Two luminescent coordination polymers as highly selective and sensitive chemosensors for Cr^{VI}-anions in aqueous medium. *Dalton Trans.* **2019**, *48*, 387–394. [[CrossRef](#)]
9. Han, M.L.; Chang, X.H.; Feng, X.; Ma, L.F.; Wang, L.Y. Temperature and pH driven self-assembly of Zn(II) coordination polymers: Crystal structures, supramolecular isomerism, and photoluminescence. *CrystEngComm* **2014**, *16*, 1687–1695. [[CrossRef](#)]
10. Li, X.Q.; Zhou, Z.; Zhang, C.C.; Zheng, Y.H.; Gao, J.W.; Wang, Q.M. Modulation of assembly and disassembly of a new tetraphenylethene based nanosensor for highly selective detection of hyaluronidase. *Sens. Actuators B Chem.* **2018**, *276*, 95–100. [[CrossRef](#)]
11. Zhou, Z.; Han, M.L.; Fu, H.R.; Ma, L.F.; Luo, F.; Li, D.S. Engineering design toward exploring the functional group substitution in 1D channels of Zn-organic frameworks upon nitro explosives and antibiotics detection. *Dalton Trans.* **2018**, *47*, 5359–5365. [[CrossRef](#)] [[PubMed](#)]
12. Dong, X.Y.; Si, C.D.; Fan, Y.; Hu, D.C.; Yao, X.Q.; Yang, Y.X.; Liu, J.C. Effect of N-donor ligands and metal ions on the coordination polymers based on a semirigid carboxylic acid ligand: Structures analysis, magnetic properties, and photoluminescence. *Cryst. Growth Des.* **2016**, *16*, 2062–2073. [[CrossRef](#)]
13. Yang, X.G.; Lu, X.M.; Zhai, Z.M.; Zhao, Y.; Liu, X.-Y.; Ma, L.-F.; Zang, S.-Q. Facile synthesis of micro-scale MOF host-guest with long-last phosphorescence and enhanced optoelectronic performance. *Chem. Commun.* **2019**, *55*, 11099–11102. [[CrossRef](#)] [[PubMed](#)]
14. Roztocki, K.; Jedrzejowski, D.; Hodorowicz, M.; Senkowska, I.; Kaskel, S.; Matoga, D. Effect of linker substituent on layers arrangement, stability, and sorption of Zn-isophthalate/acylhydrazone frameworks. *Cryst. Growth Des.* **2018**, *18*, 488–497. [[CrossRef](#)]
15. Singh, R.; Bharadwaj, P.K. Coordination polymers built with a linear bis-imidazole and different dicarboxylates: Unusual entanglement and emission properties. *Cryst. Growth Des.* **2013**, *13*, 3722–3733. [[CrossRef](#)]
16. Guo, X.Z.; Li, J.L.; Shi, S.S.; Zhou, H.; Han, S.S.; Chen, S.S. Synthesis, structure and luminescent property of a Zn(II) complex with mixed multi-N donor and 2,5-dihydroxy-terephthalic acid ligands. *Chin. J. Struct. Chem.* **2018**, *37*, 1117–1124.
17. Cui, Y.; Li, B.; He, H.; Zhou, W.; Chen, B.; Qian, G. Metal-organic frameworks as platforms for functional materials. *Acc. Chem. Res.* **2016**, *49*, 483–493. [[CrossRef](#)]
18. Wang, S.L.; Hu, F.L.; Zhou, J.Y.; Zhou, Y.; Huang, Q.; Lang, J.P. Rigidity versus flexibility of ligands in the assembly of entangled coordination polymers based on Bi- and tetra carboxylates and N-Donor ligands. *Cryst. Growth Des.* **2015**, *15*, 4087–4097. [[CrossRef](#)]
19. Wang, S.; Yun, R.; Peng, Y.; Zhang, Q.; Lu, J.; Dou, J.; Bai, J.; Li, D.; Wang, D. A series of four-connected entangled metal–organic frameworks assembled from pamoic acid and pyridine-containing ligands: Interpenetrating, self-penetrating, and supramolecular isomerism. *Cryst. Growth Des.* **2012**, *12*, 79–92. [[CrossRef](#)]

20. Chang, X.H.; Qin, J.H.; Ma, L.F.; Wang, J.G.; Wang, L.Y. Two- and three-dimensional divalent metal coordination polymers constructed from a new tricarboxylate linker and dipyridyl ligands. *Cryst. Growth Des.* **2012**, *12*, 4649–4657. [[CrossRef](#)]
21. Hernández-Maldonado, A.J.; Arrieta-Pérez, R.R.; Primera-Pedrozo, J.N.; Exley, J. Structure of a porous $\text{Cu}_2(\text{pzdc})_2(\text{bpp})$ (pzdc: Pyrazine-2,3-dicarboxylate, bpp: 1,3-Bis(4-pyridyl)propane) coordination polymer and flexibility upon concomitant hysteretic CO_2 adsorption. *Cryst. Growth Des.* **2015**, *15*, 4123–4131. [[CrossRef](#)]
22. Chen, S.S.; Chen, M.; Takamizawa, S.; Chen, M.S.; Su, Z.; Sun, W.Y. Temperature dependent selective gas sorption of the microporous metal-imidazolate framework $[\text{Cu}(\text{L})]$ [$\text{H}_2\text{L} = 1,4\text{-di}(1\text{H-imidazol-4-yl})\text{benzene}$]. *Chem. Commun.* **2011**, *47*, 752–754. [[CrossRef](#)] [[PubMed](#)]
23. Chen, S.S.; Chen, M.; Takamizawa, S.; Wang, P.; Lv, G.C.; Sun, W.Y. Porous cobalt(II)-imidazolate supramolecular isomeric frameworks with selective gas sorption property. *Chem. Commun.* **2011**, *47*, 4902–4904. [[CrossRef](#)] [[PubMed](#)]
24. Chen, S.S.; Wang, P.; Takamizawa, S.; Okamura, T.A.; Chen, M.; Sun, W.Y. Zinc(II) and cadmium(II) metal-organic frameworks with 4-imidazole containing tripodal ligand: Sorption and anion exchange properties. *Dalton Trans.* **2014**, *43*, 6012–6020. [[CrossRef](#)] [[PubMed](#)]
25. Sun, Y.X.; Sun, W.Y. Zinc(II)- and cadmium(II)-organic frameworks with 1-imidazole-containing and 1-imidazole-carboxylate ligands. *CrystEngComm* **2015**, *17*, 4045–4063. [[CrossRef](#)]
26. Chen, S.S.; Sheng, L.Q.; Zhao, Y.; Liu, Z.D.; Qiao, R.; Yang, S. Syntheses, structures, and properties of a series of polyazaheteroaromatic core-based Zn(II) coordination polymers together with carboxylate auxiliary ligands. *Cryst. Growth Des.* **2016**, *16*, 229–241. [[CrossRef](#)]
27. Have, R.T.; Huisman, M.; Meetsma, A.; van Leusen, A.M. Novel synthesis of 4(5)-monosubstituted imidazoles via cycloaddition of tosylmethyl isocyanide to aldimines. *Tetrahedron* **1997**, *53*, 11355–11368. [[CrossRef](#)]
28. SAINT; Version 6.2; Bruker AXS, Inc.: Madison, WI, USA, 2001.
29. Sheldrick, G.M. SADABS; University of Göttingen: Göttingen, Germany, 1997.
30. Sheldrick, G.M. SHELXTL; Version 6.10; Bruker Analytical Xray Systems: Madison, WI, USA, 2001.
31. Wang, C.Y.; Wilseck, Z.M.; LaDuca, R.L. $1\text{D} + 1\text{D} \rightarrow 1\text{D}$ polyrotaxane, $2\text{D} + 2\text{D} \rightarrow 3\text{D}$ interpenetrated, and 3D self-penetrated divalent metal terephthalate bis(pyridylformyl)piperazine coordination polymers. *Inorg. Chem.* **2011**, *50*, 8997–9003. [[CrossRef](#)]
32. Chen, S.S.; Li, J.L.; Li, W.D.; Guo, X.Z.; Zhao, Y. Four new transition metal coordination polymers based on mixed 4-imidazole and carboxylate-sulfonate ligands: Syntheses, structures, and properties. *J. Solid State Chem.* **2019**, *277*, 510–518. [[CrossRef](#)]
33. Xue, L.P.; Li, Z.H.; Ma, L.F.; Wang, L.Y. Crystal engineering of cadmium coordination polymers decorated with nitro-functionalized thiophene-2,5-dicarboxylate and structurally related bis(imidazole) ligands with varying flexibility. *CrystEngComm* **2015**, *17*, 6441–6449. [[CrossRef](#)]
34. Liu, X.M.; Xie, L.H.; Lin, J.B.; Lin, R.B.; Zhang, J.P.; Chen, X.M. Flexible porous coordination polymers constructed from 1,2-bis(4-pyridyl)hydrazine via solvothermal in situ reduction of 4,4'-azopyridine. *Dalton Trans.* **2011**, *40*, 8549–8554. [[CrossRef](#)] [[PubMed](#)]
35. Zhu, M.A.; Guo, X.Z.; Xiao, L.; Chen, S.S. A new Cd(II) coordination compound based on 4-(1,2,4-Triazol-4-yl)phenylacetic acid: Synthesis, structure and photoluminescence property. *Chin. J. Struct. Chem.* **2018**, *37*, 437–444.
36. Shi, Z.; Pan, Z.; Qin, L.; Zhou, J.; Zheng, H. Five new transition metal coordination polymers based on V-shaped bis-triazole ligand with aromatic dicarboxylates: Syntheses, structures, and properties. *Cryst. Growth Des.* **2017**, *17*, 2757–2766. [[CrossRef](#)]
37. Liu, L.; Huang, C.; Xue, X.; Li, M.; Hou, H.; Fan, Y. Ni(II) coordination polymers constructed from the flexible tetracarboxylic acid and different N-donor ligands: Structural diversity and catalytic activity. *Cryst. Growth Des.* **2015**, *15*, 4507–4517. [[CrossRef](#)]
38. Hu, Z.Y.; Zhao, M.; Su, J.; Xu, S.; Hu, L.; Liu, H.; Zhang, Q.; Zhang, J.; Wu, J.; Tian, Y. Three coordination polymers based on a star-like geometry 4,4'-nitrotribenzoic acid ligand and their framework dependent luminescent properties. *J. Solid State Chem.* **2018**, *258*, 328–334. [[CrossRef](#)]

